Journal of Molecular Catalysis A: Chemical 326 (2010) 21–28

Contents lists available at ScienceDirect

Journal of Molecular Catalysis A: Chemical

journal homepage: www.elsevier.com/locate/molcata

Editor's choice paper

Influence of phosphorus and oxygen donor diphosphine ligands on the reactivity of rhodium(I) carbonyl complexes

Biswajit Deb, Dipak Kumar Dutta*

Materials Science Division, North East Institute of Science and Technology (Council of Scientific and Industrial Research), Jorhat 785 006, Assam, India

ARTICLE INFO

Article history:
Received 23 February 2010
Received in revised form 12 May 2010
Accepted 14 May 2010
Available online 11 June 2010

Keywords:
Rhodium
Carbonyl complexes
Oxygen donor
Diphosphine
Carbonylation

ABSTRACT

The dimeric rhodium precursor $[Rh(CO)_2Cl]_2$ reacts with two molar equivalent of 9,9-dimethyl-4,5-bis(diphenylphosphino)xanthene [xantphos] (**a**), bis(2-diphenylphosphinophenyl)ether [DPEphos] (**b**) and their corresponding dioxide analogues xantphos dioxide (**c**), DPEphos dioxide (**d**) to afford the mono- and dicarbonyl complexes of the type [Rh(CO)Cl(L)] (**1a**,**1b**) and $[Rh(CO)_2Cl(L)]$ (**1c**,**1d**) respectively, where L = **a**–**d**. The complexes **1a**–**1d** have been characterized by elemental analyses, IR and NMR (^1H, ^{31}P and ^{13}C) spectroscopy, and the structure of the ligand **d** was determined by single crystal X-ray diffraction. **1a**–**1d** undergo oxidative addition (OA) reactions with different electrophiles such as CH_3I, C_2H_5I and I_2 to give Rh(III) complexes of the types $[Rh(CO)_y(COR)ClXL]$ {R = $-CH_3$ (**2a**–**2d**), $-C_2H_5$ (**3a**–**3d**); X = I and $y = 0$, L = **a**, **b**; $y = 1$, L = **c**, **d**} and $[Rh(CO)ClI_2L]$ (**4a**–**4d**) respectively. Kinetic data for the reactions of **1a**–**1d** with CH_3I indicate a pseudo-first-order reaction. The catalytic activity of **1a**–**1d** for the carbonylation of methanol to acetic acid and its ester was evaluated at different CO pressure 15, 20 and 33 bar at 130 °C and a higher Turn Over Number (TON) (679–1768) were obtained compared to that of the well-known commercial species $[Rh(CO)_2I_2]^-$ (TON = 463–1000) in each case under the similar experimental conditions.

1. Introduction

Oxidative addition to organometallic compounds is one of the key elementary steps in many catalytic processes. For this reason, the reaction has been extensively studied, and in the last few years many publications have appeared concerning its implication to ligand-promoted methanol carbonylation to acetic acid production [1–17]. The original $[Rh(CO)_2I_2]^-$ catalyst, developed at the Monsanto's laboratories [18] and studied in detail by Forster and co-workers [19,20], is largely used for the industrial production of acetic acid. It is commonly accepted that the rate determining step of this reaction is precisely the oxidative addition of MeI to a square planar d^8 complex [21] and therefore the major focus has been made on the design of catalysts for the improvement of this reaction. Ligands that increase the electron density at the metal center should facilitate the oxidative addition step and, consequently, increase the overall rate of acetic acid formation.

For this purpose, a large variety of rhodium carbonyl complexes have been synthesized by incorporating different ligands into its coordination sphere and evaluated for methanol carbonylation, giving comparable or better activities compared to the original Monsanto's catalyst [1–17,22–24]. As a part of our continuing research activity [13–17,25–27], we have chosen two diphosphine ligands viz. 9,9-dimethyl-4,5-bis-(diphenylphosphino)xanthene (xantphos) and bis(2-diphenylphosphinophenyl)ether (DPEphos) with different ligand backbone and made them oxygen functionalized by oxidation of the phosphorus atoms. In this paper, we report the synthesis of four rhodium(I) carbonyl complexes containing the 'Soft' (phosphorus) and 'Hard' (oxygen) donor diphosphine ligands and their reactivity with different electrophiles like CH_3I, C_2H_5I and I_2. The effects of backbone and donor capacity of the ligands on catalytic carbonylation of methanol under different CO pressure have also been studied.

2. Experimental

2.1. General definition

All solvents were distilled under N_2 prior to use. $RhCl_3 \cdot xH_2O$ was purchased from M/S Arrora Matthey Ltd., Kolkota, India. The ligands xantphos and DPEphos were purchased from Across Organics, Belgium and used without further purification. H_2O_2 was obtained from Ranbaxy, New Delhi, India and estimated before use.

Elemental analyses of C and H were performed on a Perkin-Elmer 2400 elemental analyzer. The elements P, Cl and Rh were analyzed quantitatively by standard analytical techniques [28,29],

* Corresponding author. Tel.: +91 376 2370081; fax: +91 376 2370011.
E-mail address: dipakkrdutta@yahoo.com (D.K. Dutta).

1381-1169/$ – see front matter © 2010 Elsevier B.V. All rights reserved.
doi:10.1016/j.molcata.2010.05.008

and the quantity of O was determined by difference. IR spectra (4000–400 cm^{-1}) were recorded in KBr discs and $CHCl_3$ on a Perkin-Elmer system 2000 FT-IR spectrophotometer. The ^1H, ^{13}C and ^{31}P NMR spectra were recorded at room temperature in $CDCl_3$ solution on a Bruker DPX-300 Spectrometer and chemical shifts were reported relative to $SiMe_4$ and 85% H_3PO_3 as internal and external standards respectively. Mass spectra of the complexes were recorded on ESQUIRE 3000 Mass Spectrometer. The carbonylation reactions of methanol were carried out in a high pressure reactor (Parr-4592, USA) fitted with a pressure gauge and the reaction products were analyzed by GC (Chemito 8510, FID).

2.2. Synthesis of xantphos dioxide (**c**) and DPEphos dioxide (**d**)

The ligands xantphos and DPEphos dioxide were synthesized by oxidation of xantphos and DPEphos respectively by H_2O_2 following the literature protocol [25,27]

Analytical data:

Xantphos dioxide (**c**)

IR (KBr, cm^{-1}): 1193 [ν(P–O)]. ^1H NMR ($CDCl_3$, ppm): δ 6.74–7.74 (m, 30H, Ph), 2.17 (s, 6H, CH_3). ^{13}C NMR ($CDCl_3$, ppm): δ 153.10–124.1 (m, Ar), δ 32.3, 34.9 (s, CH_3). $^{31}P\{^1H\}$ NMR ($CDCl_3$, ppm): δ 30.95 [s, P=O]. Elemental analyses; Found (Cald. for $C_{39}H_{32}O_3P_2$): C 73.98 (74.40); H 5.02 (5.08).

DPEphos dioxide (**d**)

IR (KBr, cm^{-1}): 1198, 1186 [ν(P–O)]. ^1H NMR (DMSO-D_6, ppm): δ 6.11–6.18, 7.2–7.69 (m, 28H, Ar), ^{13}C NMR (DMSO-D_6, ppm): δ 122.5–134.21 (m, Ar), δ 153.4 (s, O–C_{phenyl}). $^{31}P\{^1H\}$NMR (DMSO-D_6, ppm): δ 26.21, 24.21 [s, P=O]. Elemental analyses; Found (Cald. for $C_{36}H_{28}O_3P_2$): C 75.18 (75.71); H 4.73 (4.90).

2.3. Synthesis of starting material

$[Rh(CO)_2Cl]_2$ was prepared by passing CO gas over $RhCl_3{\cdot}3H_2O$ at 100 °C in the presence of moisture [30].

2.4. Synthesis of the complexes $[Rh(CO)_xClL]$ (**1a**–**1d**), where L = xantphos (**a**), DPEphos (**b**) and x = 1; L = xantphos dioxide (**c**), DPEphos dioxide (**d**) and x = 2

$[Rh(CO)_2Cl]_2$ (100 mg) was dissolved in dichloromethane (10 cm^3) and to that solution, a stoichiometric quantity (Rh:L = 1:1) of the respective ligands were added. The reaction mixture was stirred at room temperature (r.t.) for about 10–60 min and the solvent was evaporated under vacuum. The yellowish red coloured compounds so obtained were washed with diethyl ether and stored over silica gel in a desiccator.

Analytical data for the complexes **1a**–**1d** are given as follows:

*[Rh(CO)Cl(Xantphos)] (**1a**)*

IR (KBr, cm^{-1}): 1974 [ν(CO)]. ^1H NMR ($CDCl_3$, ppm): δ 6.82–7.09, 7.31–7.88 (m, Ph), δ 1.69 (s, CH_3). ^{13}C NMR ($CDCl_3$, ppm): δ 152.2–126.5 (m, Ar), δ 63.8 (CMe_2), δ 32.5 (s, CH_3), δ 183.3 (s, CO). $^{31}P\{^1H\}$ NMR ($CDCl_3$, ppm): δ 22.55 [d, J_{P-Rh} = 123.5 Hz]. Elemental analyses: Found (Cald. for $C_{40}H_{32}O_2P_2ClRh$), C 63.85 (64.48); H 4.21 (4.30); P 8.45 (8.32); Cl 4.89 (4.77); Rh 13.72 (13.82); O 4.88 (4.30).

*[Rh(CO)Cl(DPEphos)] (**1b**)*

IR (KBr, cm^{-1}): 1985 [ν(CO)]. ^1H NMR ($CDCl_3$, ppm): δ 6.80–7.20, 7.30–7.37, 7.54–7.79 (m, Ph). ^{13}C NMR ($CDCl_3$, ppm): δ 154.8–128.2 (m, Ar), δ 180.9 (s, CO). $^{31}P\{^1H\}$ NMR ($CDCl_3$, ppm): δ 27.3 [d, J_{P-Rh} = 119.2 Hz]. Elemental analyses: Found (Cald. for $C_{37}H_{28}O_2P_2ClRh$), C 62.91 (63.06); H 3.73 (3.97); P 8.85 (8.79); Cl 5.15 (5.04); Rh 14.23 (14.61); O 5.13 (4.54).

*[$Rh(CO)_2$Cl(Xantphos dioxide)] (**1c**)*

IR (KBr, cm^{-1}): 1983, 2058 [ν(CO)], 1190, 1185 [ν(P=O)]. ^1H NMR ($CDCl_3$, ppm): δ 6.68–7.61 (m, Ph), δ 1.69 (s, CH_3). ^{13}C NMR ($CDCl_3$, ppm): δ 153.8–125.2 (m, Ar), δ 34.23 (s, CH_3), δ 178.5, 180.3 (s, CO). $^{31}P\{^1H\}$ NMR ($CDCl_3$, ppm): δ 45.5 (d, J_{P-P} = 69.2 Hz), δ 48.04 (d, J_{P-P} = 69.2 Hz). Elemental analyses: Found (Cald. for $C_{41}H_{32}O_5P_2ClRh$), C 60.73 (61.17); H 3.78 (3.98); P 8.01 (7.70); Cl 4.59 (4.41); Rh 12.60 (12.79); O 10.29 (9.94).

*[$Rh(CO)_2$Cl(DPEphos dioxide)] (**1d**)*

IR (KBr, cm^{-1}): 1996, 2071 [ν(CO)], 1189, 1186 [ν(P=O)]. ^1H NMR (DMSO-D_6, ppm): δ 6.15–6.38, 7.11–7.82 (m, Ph). ^{13}C NMR (DMSO-D_6, ppm): δ 119.2–138.5 (m, Ar), δ 153.8 (s, O–C_{phenyl}), δ 182.5, 185.9 (s, CO). $^{31}P\{^1H\}$ NMR (DMSO-D_6, ppm): δ 35.8, 24.7 (s, P=O). Elemental analyses: Found (Cald. for $C_{38}H_{28}O_5P_2ClRh$), C 58.98 (59.65); H 3.51 (3.66); P 8.32 (8.10); Cl 4.41 (4.64); Rh 13.82 (13.46); O 10.96 (10.47).

2.5. Reactivity of $[Rh(CO)ClL]$ (**1a**,**1b**) and $[Rh(CO)_2ClL]$ (**1c**,**1d**) with CH_3I, C_2H_5I and I_2

2.5.1. Synthesis of $[Rh(CO)_y(COR)ClXL]$ R = CH_3, X = I, y = 0 (**2a**,**2b**), y = 1 (**2c**,**2d**); R = C_2H_5, X = I, y = 0 (**3a**,**3b**), y = 1(**3c**,**3d**)

$[Rh(CO)_2ClL]$ (50 mg) was dissolved in dichloromethane (5 cm^3) and each of RX (3 cm^3) (RX = CH_3I, C_2H_5I) was added to it. The reaction mixture was then stirred at r.t. for about 2–10 h for CH_3I and C_2H_5I respectively. The colour of the solution changed from yellowish red to dark reddish brown and the solvent was evaporated under vacuum. The compounds so obtained were washed with diethyl ether and stored over silica gel in a desiccator.

2.5.2. Synthesis of $[Rh(CO)ClI_2L]$ (**4a**–**4d**)

$[Rh(CO)_2ClL]$ (50 mg) was dissolved in CH_2Cl_2 (15 cm^3) and to this solution I_2 (25 mg) was added. The reaction mixture was then stirred at r.t. for about 4 h. The solvent was evaporated under vacuum and the brown coloured compound so obtained were washed with hexane and stored over silica gel in a desiccator.

2.6. X-ray structural analysis

Single crystal of **d** was grown by slow evaporation of a saturated solution of **d** in acetone. The intensity data of the compounds were collected on Bruker Smart–CCD with Mo Kα radiation (λ = 0.71073 Å) at 293 K. The structure was solved with SHELXS-97 and refined by full-matrix least squares on F^2 using SHELXL-97 computer program [31]. Hydrogen atoms were idealized by using the riding models.

2.7. Kinetic experiment

The kinetic experiments of OA reaction of complexes **1a**–**1d** with CH_3I were monitored using FT-IR spectroscopy in a solution cell (CaF_2 windows, 1.0 mm path length). In order to obtain pseudo-first-order condition, excess of CH_3I relative to metal complex was used. FT-IR spectra (4.0 cm^{-1} resolution) were scanned in the ν(CO) region (2200–1600 cm^{-1}) and saved at regular time interval using spectrum software. After completion of experiment, absorbance versus time data for the appropriate ν(CO) frequencies were extracted by subtracting the solvent spectrum and analyzed off line using OriginPro 7.5 software. Kinetic measurements were made by following the decay of lower frequency ν(CO) band of the complexes in the region 1974–1996 cm^{-1}. The pseudo-first-order rate constants were found from the gradient of the plot of $\ln(A_o/A_t)$ versus time, where A_o is the initial absorbance and A_t is the absorbance at time t.

2.8. Carbonylation of methanol using complexes **1a**–**1d** as catalyst precursors

CH_3OH (0.099 mol, 4 cm^3), CH_3I (0.016 mol, 1 cm^3), H_2O (0.055 mol, 1 cm^3) and catalyst (0.0514 mmol) were placed in a

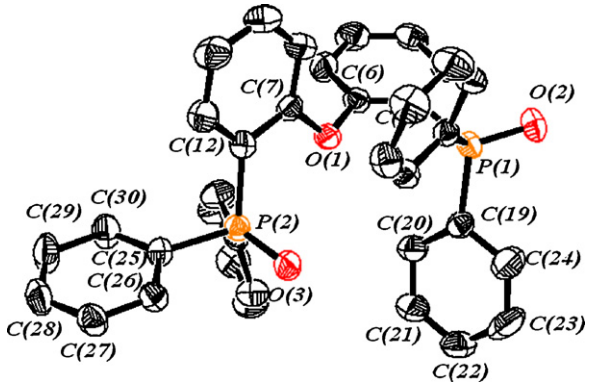

Fig. 1. X-ray crystal structure of the ligand **d**.

50 mL reaction vessel. The reaction mixture was then purged with CO for about 5 min and then pressurized with CO gas at around 5, 10 and 20 bar respectively at 25 °C. The carbonylation reactions were carried out at 130 ± 2 °C for 1 h with corresponding gas pressure at around 15 ± 2, 20 ± 2 and 33 ± 2 bar. The products were collected and analyzed by G.C.

Table 1
Crystallographic data and selected bond lengths for the ligand **d**.

Crystallographic information	
Empirical formula	$C_{36}H_{28}O_3P_2$
Formula weight	570.5
Temperature (K)	293
λ (Å)	0.71073
Cryst. Syst.	Triclinic
Space group	*Pbca*
Z	8
a (Å)	18.2628 (4)
b (Å)	15.0368 (3)
c (Å)	21.3338 (4)
α (°)	90
β (°)	90
γ (°)	90
μ(Mo Kα) mm^{-1}	0.184
Reflections collected	5647
R1 (observed data)	0.0466 (3982)
wR2 (all data)	0.1132 (5647)
Selected bond lengths (Å)	
P(1)–O(2)	1.4822 (16)
P(2)–O(3)	1.4803 (15)
O(3)···O(2) (Spatial)	6.414

3. Results and discussion

3.1. Single crystal X-ray structural determination of *d*

The single crystal X-ray structure of xantphos dioxide (**c**) was previously determined by us [25], only the crystal structure of DPEphos dioxide (**d**) ligand is reported in this paper (Fig. 1). The crystal information of **d** and the selected bond lengths are summarized in Table 1. The compound **d** crystallizes in a triclinic system with space group *Pbca*. The average P–O bond length (1.48 Å) of **d** is similar to the P=O bond lengths reported in literature [13,25]. The ligand **d** exhibits interesting intermolecular interactions involving shorter distances than the sum of van der Waals radii (Fig. 2). The interactions between these molecules are presented by dotted lines and summarized in Fig. 2. The molecules are connected by weak hydrogen bonding between H atoms of the phenyl ring and O atom of P=O group (C–H···O=P) of the adjacent molecules [C(26)–H(26)···O(2) 2.512 Å] to develop an extended one dimensional network (Fig. 2).

3.2. Synthesis and characterization of *1a–1d*

The reaction of the chloro-bridge dimer $[Rh(CO)_2Cl]_2$ with two molar equivalent of 9,9-dimethyl-4,5-bis(diphenylphosphino) xanthene [xantphos] (**a**) and bis(2-diphenylphosphinophenyl) ether [DPEphos] (**b**) in dichloromethane proceeds rapidly with the evolution of CO gas to yield the monocarbonyl complexes of the type [Rh(CO)Cl(L)] (**1a**,**1b**) where L = **a**, **b** (Scheme 1). Elemental analyses of the complexes support the observed molecular composition of **1a** and **1b**. The IR spectra of **1a** and **1b** exhibit single intense ν(CO) bands at around 1974 and 1985 cm^{-1} respectively indicate the formation of monocarbonyl rhodium(I) complexes of diphosphine ligands. The complexes **1a** and **1b** show characteristic $^{31}P\{^1H\}$ NMR spectra with doublet at around δ 22.55 (d, J_{P-Rh} = 123.5 Hz) and 27.3 (d, J_{P-Rh} = 119.2 Hz) ppm respectively and ^1H NMR spectra with phenylic multiplet in the range δ 6.80–7.88 ppm. Thus, $^{31}P\{^1H\}$ NMR spectra show downfield shift compared to the free ligands (δ −16.3 (**a**) and −12.1 (**b**) ppm) indicating chelate formation through phosphorus donor. The ^{13}C NMR spectra of **1a** and **1b** show characteristic resonances at around δ 183 and 181 ppm respectively for the carbonyl carbons. The phenyl and other carbons in the complexes are found in their respective ranges. On the other hand, the dimeric precursor $[Rh(CO)_2Cl]_2$ reacts with dioxide analogues of **a** and **b** i.e. xantphos dioxide (**c**) and DPEphos dioxide (**d**) in CH_2Cl_2 to yield the dicarbonyl complexes of the type $[Rh(CO)_2Cl(L)]$ (**1c**,**1d**) where L = **c**, **d** (Scheme 1). The IR spectra of **1c** and **1d** exhibit two intense ν(CO) bands in the range 1983–2071 cm^{-1} indicating the presence of two terminal CO groups. The ν(P–O) bands of the complexes at around 1190, 1185 (**1c**) and 1189, 1186 (**1d**) cm^{-1} respectively are lower than those of the corresponding free ligands [ν(P–O) = 1193 (**c**) and 1198, 1186 (**d**) cm^{-1}] confirming the formation of Rh–O bonds. The complexes **1c** and **1d** show characteristic $^{31}P\{^1H\}$ NMR spectra with two doublets at around δ 45.5, 48.04 (d, J_{P-P} = 69.2 Hz) and singlets

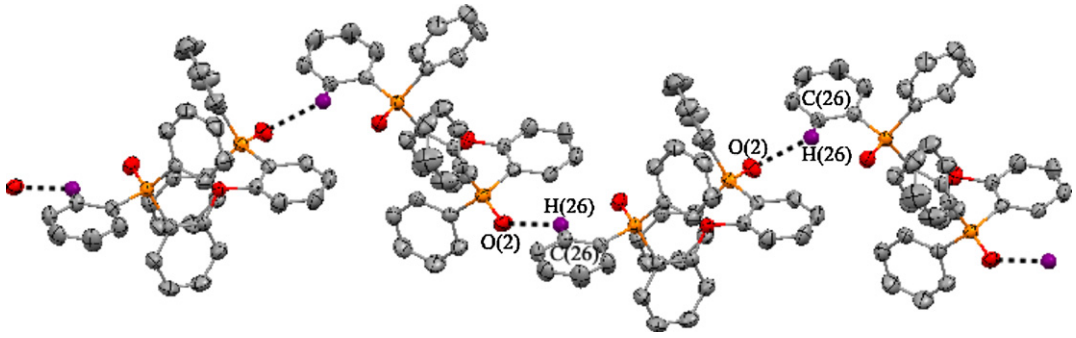

Fig. 2. Extended one dimensional network of **d** down the crystallographic *c*-axis stabilized through C–H···O [C(36)–H(36)···O(2) 2.512 Å] hydrogen bonding.

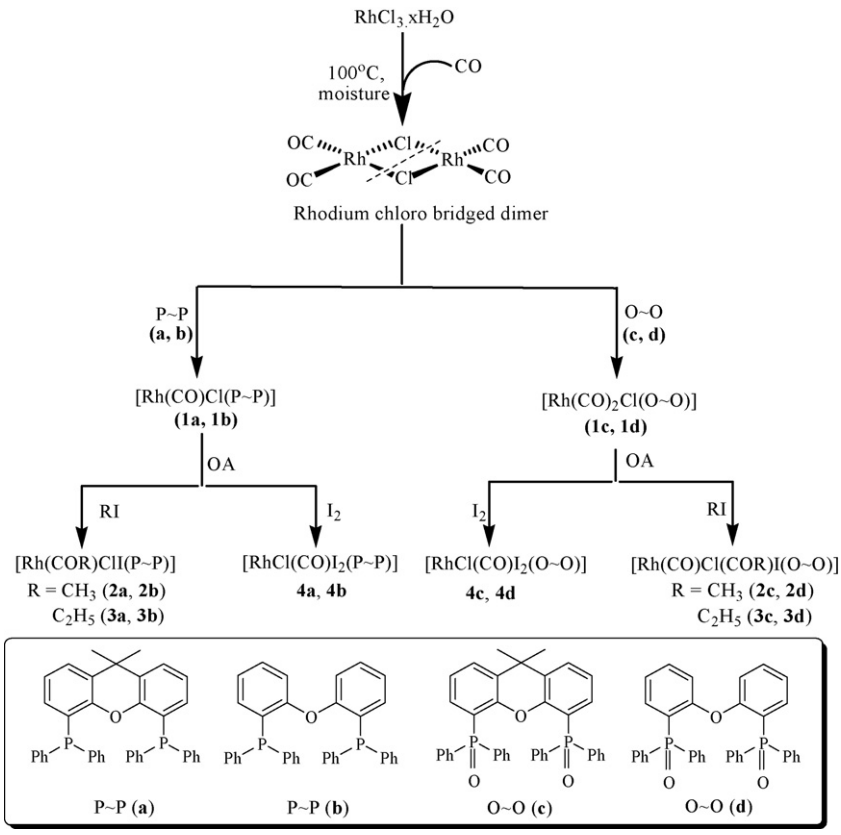

Scheme 1. Synthesis and reactivity of **1a**–**1d**.

at around δ 24.7, 35.8 ppm respectively and also ^{1}H NMR spectra with phenylic multiplet in the range δ 6.15–7.82 ppm. The occurrence of lower ν(P–O) bands in **1c** and the downfield shift of the $^{31}P\{^{1}H\}$ NMR spectrum suggesting the formation of chelate complex. However, in the complex **1d**, the appearance of IR band at around 1186 cm^{-1} due to uncoordinated P=O donor together with the $^{31}P\{^{1}H\}$ NMR band at around δ 24.7 ppm indicate the presence of dangling P–O group in the complex. The observed diversity of coordination mode of the two dioxide ligands during complexation under the similar experimental condition depends exclusively on their inherent structural behaviour which may be partially substantiated from the single crystal X-ray structures of **c** [25] and **d** as shown in Figs. 3 and 1 respectively. The ^{13}C NMR spectra of **1c** and **1d** show characteristic resonances for CO groups in the region δ 178–186 ppm along with other characteristic bands of the coordinated ligands. It is interesting to mention here that the rhodium dicarbonyl precursor reacts with **a**, **b** to form monocarbonyl complexes, while, the dioxide analogues **c**, **d** under similar reaction condition afford dicarbonyl complexes. This fact may be due to the moderate π accepting tendency of PPh_2 moiety of **a**, **b** which compete with the coordinated CO groups facilitating decarbonylation to stabilize the monocarbonyl complexes, while, the oxygen donor ligands (**c**, **d**) act as only σ donor and favour to generate dicarbonyl complexes.

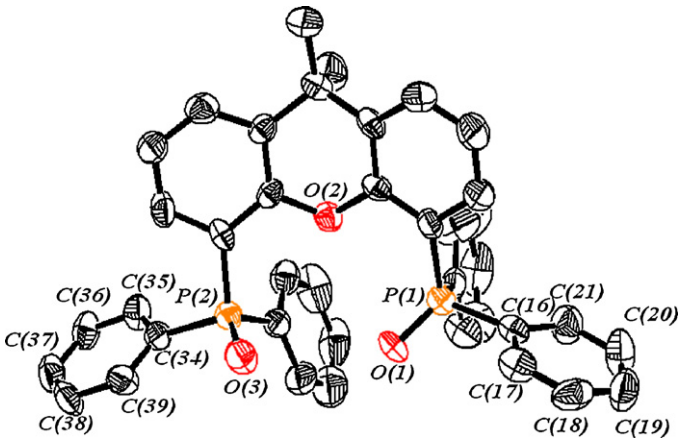

Fig. 3. X-ray crystal structure of the ligand **c**. Selected bond lengths (Å): P(2)–O(3) 1.479(4), P(1) O(1) 1.476(4), O(1)···O(3) (spatial) 3.374

3.3. *Reactivity of **1a**–**1d** towards various electrophiles*

One of the most important industrial processes utilizing homogeneous transition-metal catalysis is the rhodium and iodide promoted carbonylation of methanol to acetic acid. In this respect, OA reaction of alkyl halides with metal complexes is a very important reaction as it is the key step in the carbonylation catalysis [32]. Therefore, oxidative reactivities of **1a**–**1d** towards various electrophiles were evaluated.

The complexes **1a**–**1d** undergo OA reactions with CH_3I and C_2H_5I to generate Rh(III) complexes of the type [RhCl(CO)$_y$(COR)IL], where R = –CH_3, y = 0 (**2a**,**2b**) and y = 1 (**2c**,**2d**); R = –C_2H_5 (**3a**,**3b**), y = 0 (**3a**,**3b**) and y = 1 (**3c**,**3d**) (Scheme 1). On the other hand, **1a**–**1d** reacts with I_2 in dichloromethane to produce Rh(III) complexes of the type [RhCl(CO)I_2L] (**4a**–**4d**) (Scheme 1). The IR spectra of the oxidized products show single characteristic terminal ν(CO) bands in the range 2038–2075 cm^{-1} and a broad ν(CO) band (except **4a**–**4d** in which the electrophile is iodine) in the range 1678–1733 cm^{-1} characteristic of acyl carbonyl groups (Table 2). The ^{1}H NMR spectra of the complexes **2a**–**2d** display singlet resonances in the range δ 2.58–2.78 ppm suggesting the formation of –OCCH$_3$ group

Table 2
Significant IR, ^{1}H and ^{13}C NMR data for the oxidative addition (OA) adducts.

OA adducts	IR (cm^{-1})		^{1}H NMR (ppm)		^{13}C NMR (ppm)	
	$\nu(CO)_t$	$\nu(CO)_{acyl}$	CH_3	CH_2	$(CO)_t$	$(CO)_{acyl}$
2a	–	1678	1.63(s) 2.78(s)	–	–	206(s)
2b	–	1702	2.62(s)	–	–	205.6(s)
2c	2044	1709 1733	1.68(s) 2.58(s)	–	181.5(s)	203.4(s)
2d	2057	1719	2.72(s)	–	182.5(s)	204.1(s)
3a	–	1727	1.73(s) 1.21(t)	3.56(q)	–	201.4(s)
3b	–	1691	1.13(t)	3.57(q)	–	204.8(s)
3c	2038	1725	1.78(s) 1.22(t)	3.42(q)	184.5(s)	206.2(s)
3d	2057	1713	1.19(t)	3.24(q)	180.3(s)	207.6(s)
4a	2071	–	1.68(s)	–	185.6(s)	–
4b	2074	–	–	–	184.3(s)	–
4c	2075	–	1.76(s)	–	183.4(s)	–
4d	2068	–	–	–	188.6(s)	–

including other characteristic bands of the ligands. Similarly, the complexes **3a**–**3d** shows the bands for methylene and methyl protons of $-OCCH_2CH_3$ group as quartet and triplet respectively in the range δ 1.13–3.57 ppm (Table 2). The ^{13}C NMR spectra of **2a**–**2d** and **3a**–**3d** exhibit bands in the range 201–208 ppm characteristic of the acyl carbonyl group.

Attempts to substantiate the structures of different rhodium(I) and rhodium(III) carbonyl complexes by X-ray crystal structure determination were not possible because no suitable crystals could be obtained in spite of numerous attempts.

Kinetic measurements for the OA reaction of the complexes **1a**–**1d** with methyl iodide were carried out using IR spectroscopy by monitoring the changes in the ν(CO) band(s). Fig. 4 shows a typical series of spectra of **1c** when reacts with CH_3I at 25 °C, in which the bands at around 1983 and 2058 cm^{-1} decay and new bands grow in the region 2040–2070 and 1700–1750 cm^{-1}. Finally, the two terminal ν(CO) bands at around 2058 and 1983 cm^{-1} of **1c** are replaced by two new terminal ν(CO) bands 2044 (intense) and 2067 (weak) cm^{-1} and two broad acyl ν(CO) bands at around 1709 and 1733 cm^{-1}. The presence of two acyl ν(CO) bands of almost equal intensity may be due to the formation of equimolar quantity of two acyl Rh(III) complexes in the reaction mixture as shown in Scheme 2. Absorbance versus time plots for the decay of lower intensity ν(CO) bands at 1974, 1985, 1983 and 1996 cm^{-1} of **1a**–**1d** respectively are shown in Fig. 5. A linear fit of pseudo-first order was observed for the entire course of the reaction of CH_3I with the complexes **1a**–**1d** as is evidenced from the plot of $\ln(A_o/A_t)$ versus time, where A_o and A_t are the absorbance at time $t = 0$ and t, respectively (Fig. 6). From the slopes of the plots, the rate constants were calculated and found as 3.19×10^{-4}, 3.44×10^{-4}, 6.14×10^{-4} and 1.51×10^{-3} S^{-1} for the complexes **1a**, **1b**, **1c** and **1d** respectively. The rate of oxidative addition of the four complexes varies as **1a** < **1b** < **1c** < **1d**. The observed values of the rate constants indicate that the rate of OA is higher in case of dicarbonyl complexes of oxygen donor ligands than those of monocarbonyl phosphine donor complexes.

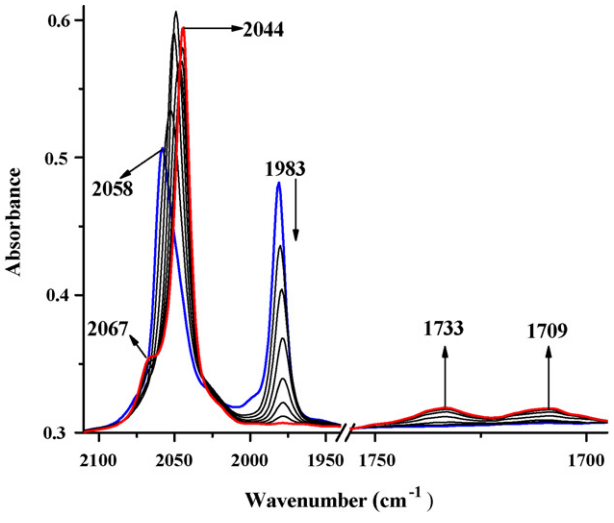

Fig. 4. Series of IR spectra {ν(CO) region} illustrating the reaction of **1c** with CH_3I at 25 °C. The arrows indicate the behaviour of each band as the reaction progresses.

3.4. Carbonylation of methanol to acetic acid and ester using the complexes *1a*–*1d* as the catalyst precursors

The results of carbonylation of methanol to acetic acid and methyl acetate in the presence of **1a**–**1d** as catalyst precursors are shown in Table 3. The precursor complexes **1a**–**1d** show total conversion of CH_3OH in the range 35.3–91.9% at 130 ± 2 °C under initial CO pressure 5–20 bar (at ~25 °C) for 1 h reaction time with corresponding TON 679–1768. It has been observed from Table 3, that as the applied CO pressure increases from 5 to 20 bar for **1a**, total conversion increases from 35.3 to 82.4% with corresponding increase in TON from 679 to 1585. Like **1a**, the complexes **1b**–**1d** also show a similar increasing trend with the increase in CO pressure and maximum TON of about 1637 (**1b**), 1718 (**1c**), and 1768 (**1d**) with corresponding conversions of 85.1, 89.3, and 91.9% have been obtained at 20 bar initial CO pressure (~25 °C). It is interesting to note that with increase of initial CO pressure, the selectivity of the catalyst changes i.e. at 5 bar CO pressure, the major product was methyl acetate; while at around 20 bar initial CO pressure, the major product was acetic acid. Under the similar experimental conditions, the well-known precursor $[Rh(CO)_2I_2]^-$ generated *in situ* from $[Rh(CO)_2Cl]_2$ [33] shows lower TON compared to **1a**–**1d**. Thus, the efficiency of the complexes depends on the nature of the ligands and follows the order **1d** > **1c** > **1b** > **1a** > $[Rh(CO)_2Cl]_2$. The observed trend is also well supported by their kinetic experiments. The monocarbonyl complexes **1a** and **1b** undergo OA of methyl

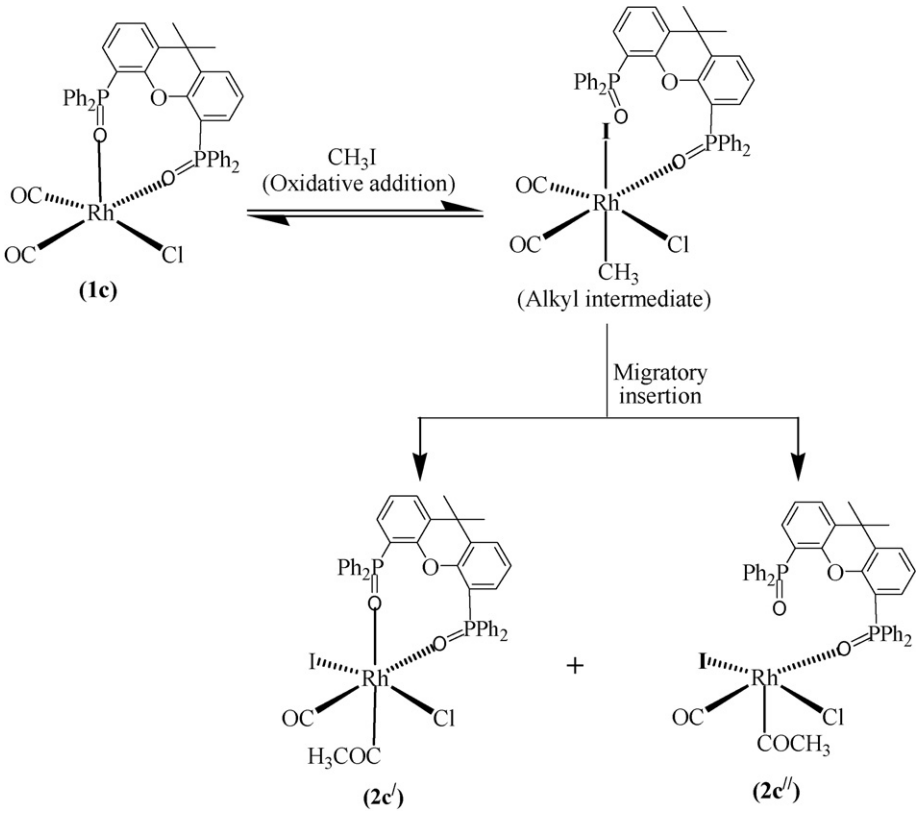

Scheme 2. Plausible Rh(III) acyl complexes (**2c**′ and **2c**″) generated after OA of CH_3I to **1c**.

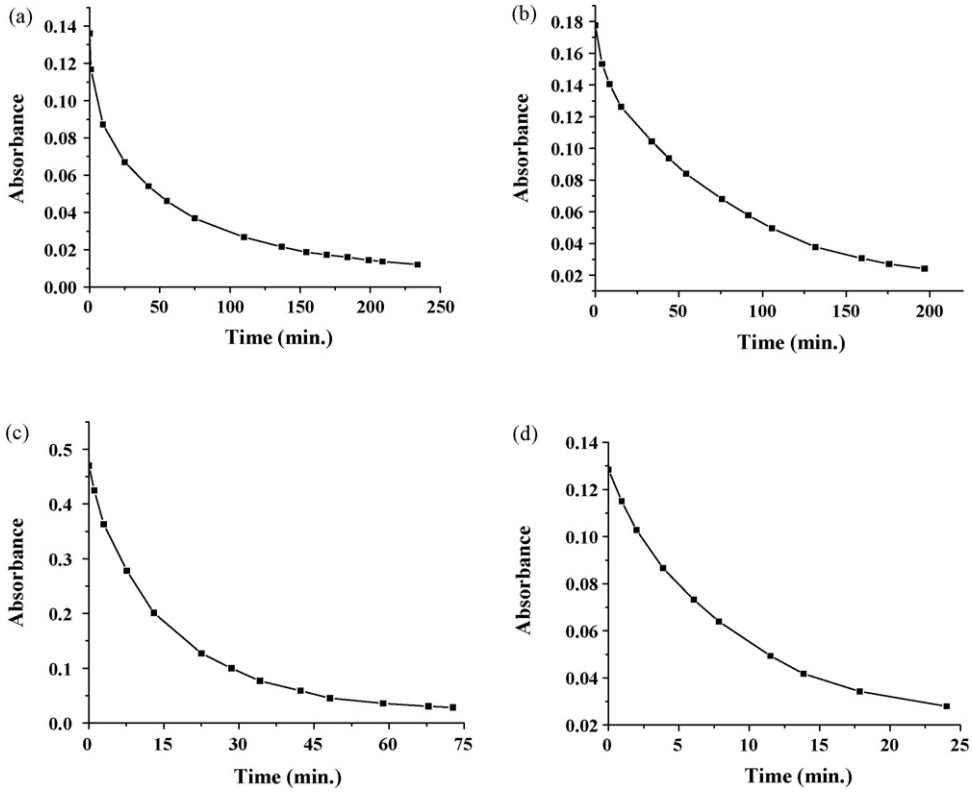

Fig. 5. Kinetic plot of (a)–(d) showing the decay of ν(CO) bands of **1a**–**1d** respectively during the reaction with neat CH_3I at room temperature (~25 °C).

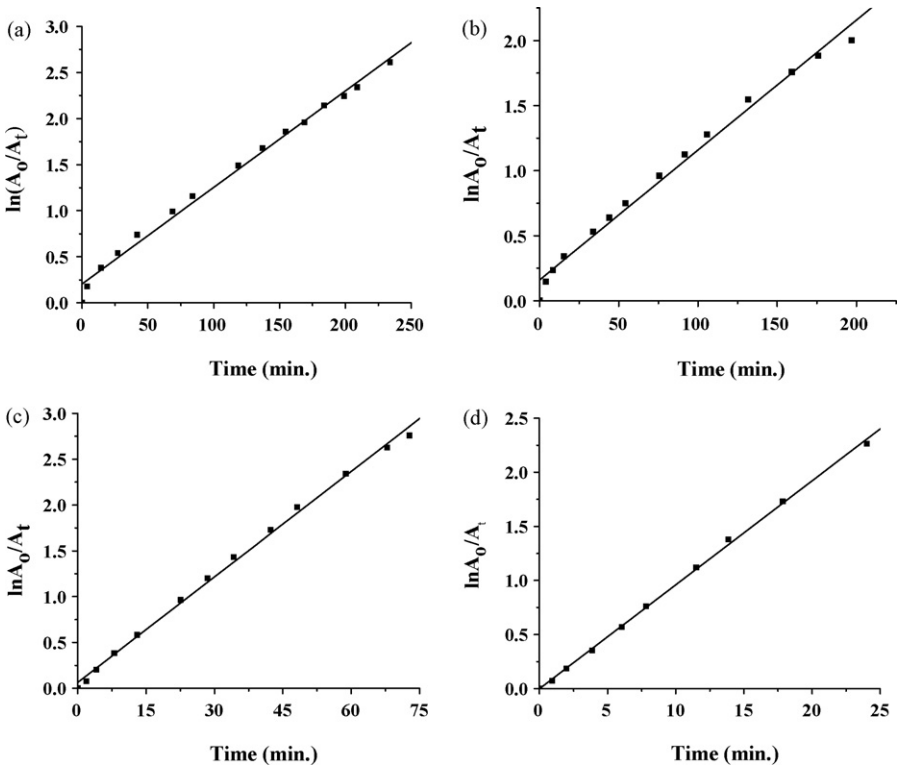

Fig. 6. $\ln(A_o/A_t)$ versus time plot in (a)–(d) are presented for the OA reaction of the complexes **1a**–**1d** respectively with neat CH_3I at ~25 °C.

Table 3
Results of methanol carbonylation.

Catalyst precursor	CO pressure at 25 °C (±1 bar)	Total conv. (%)	Acetic acid[a] (%)	Methyl acetate[a]	TON[b]
$[Rh(CO)_2I_2]^-$[c]	5	24.1	4.0	20.1	463.6
	10	41.4	12.3	29.1	796.4
	20	52.1	10.3	41.8	1000
1a	5	35.3	8.9	26.4	679.0
	10	56.2	24.0	32.2	1081.0
	20	82.4	42.1	40.3	1585.0
1b	5	36.5	7.5	29.0	702.1
	10	66.5	25.3	41.2	1279.2
	20	85.1	48.5	36.6	1637.0
1c	5	42.5	12.1	30.4	839.1
	10	66.9	27.8	39.1	1286.9
	20	89.3	49.5	39.8	1717.8
1d	5	55.2	12.6	42.6	1061.8
	10	72.4	30.4	42.0	1392.7
	20	91.9	54.4	37.5	1768.4

[a] Yield of methyl acetate and acetic acid were obtained from GC analyses after 1 h reaction time.
[b] TON = [amount of product (mol)]/[amount of catalyst (Rh mol)].
[c] Formed from added $[Rh(CO)_2Cl]_2$ under catalytic condition.

iodide with slower rate than those of dicarbonyl complexes **1c** and **1d** and hence the former show lower TON compared to latter. However, the catalytic efficiency of **1b** and **1d** is found to be higher than the similar type of complexes **1a** and **1c** respectively under identical experimental conditions, which may be due to the flexible ligand backbone of **1b** and **1d**. Such advantage of flexible ligand backbone in catalytic reaction is also reported in literature [26,34–36]. On examining the catalytic reaction mixture by IR spectroscopy at different time intervals and at the end of the catalytic reaction, multiple ν(CO) bands are obtained that matched well with the ν(CO) values of solution containing a mixture of the parent rhodium(I) carbonyl complexes **1a**–**1d** and rhodium(III) acyl complexes **2a**–**2d**. Thus, it may be inferred that the ligands remained bound to the metal center throughout the entire course of the catalytic reactions.

4. Conclusions

The new complexes of the type [Rh(CO)Cl(L)] (**1a**,**1b**) and $[Rh(CO)_2Cl(L)]$ (**1c**,**1d**) where L = **a**–**d** have been synthesized and characterized, and the structure of the ligand **d** was determined by single crystal X-ray diffraction. The complexes **1a**–**1d** undergo oxidative addition with different electrophiles like CH_3I, C_2H_5I and I_2 to afford acyl Rh(III) complexes. The kinetic data for the OA reactions with CH_3I indicate a first order reaction and also exhibit that the rate of OA for the monocarbonyl complexes **1a**, **1b** is slower

than those of dicarbonyl complexes **1c**, **1d**. The catalytic activities of **1a**–**1d** for the carbonylation of methanol to acetic acid and its ester exhibit higher TON (679–1768) than that of the well-known commercial species $[Rh(CO)_2I_2]^-$ (TON = ~464–1000) under similar experimental conditions.

Supplementary data

CCDC-699237(**d**) contains the supplementary crystallographic data for this paper. These data can be obtained free of charge via http://www.ccdc.cam.ac.uk/conts/retrieving.html, or from the Cambridge Crystallographic Data Centre, 12 Union Road, Cambridge CB2 1EZ, UK; fax: (+44) 1223 336 033; e-mail: deposit@ccdc.cam.ac.uk.

Acknowledgements

The authors are grateful to Dr. P.G. Rao, Director, North East Institute of Science and Technology (CSIR) Jorhat-785 006, Assam, India for his kind permission to publish the work. The Department of Science and Technology (DST), New Delhi (Grant: SR/S1/IC-05/2006) is acknowledged for the partial financial grant. The author B. Deb thanks to CSIR, New Delhi for providing the Senior Research Fellowship.

References

[1] J.R. Dilworth, J.R. Miller, N. Wheatly, M.J. Baker, J.G. Sunley, J. Chem. Soc., Chem. Commun. (1995) 1579–1581.
[2] P.M. Maitlis, A. Haynes, G.J. Sunley, M.J. Howard, J. Chem. Soc., Dalton Trans. (1996) 2187–2196.
[3] M.J. Baker, M.F. Giles, A.G. Orpen, M.J. Taylor, R.J. Watt, J. Chem. Soc., Chem. Commun. (1995) 197–198.
[4] M.J. Howard, M.D. Jones, M.S. Roberts, S.A. Taylor, Catal. Today 18 (1993) 325–354.
[5] A.J. Pardey, C. Longo, Coord. Chem. Rev. 254 (2010) 254–272.
[6] Z. Freixa, P.C.J. Kamer, M.L. Anthony, P.W.N.M. van Leeuween, Angew. Chem. Int. Ed. 44 (2005) 4385–4388.
[7] C.M. Thomas, R. Mafua, B. Therrien, E. Rusanov, H.S. Evans, G. Suss-Fink, Chem. Eur. J. 8 (2002) 3343–3352.
[8] S. Burger, B. Therrien, G. Suss-Fink, Helvet. Chim. Acta 88 (2005) 478–486.
[9] C.M. Thomas, G. Suss-Fink, Coord. Chem. Rev. 243 (2003) 125–142.
[10] J.F. Roth, J.H. Craddock, A. Hershman, F.E. Paulik, Chem. Technol. (1971) 600–605.
[11] K.K. Robinson, A. Hershman, J.H. Craddock, J.F. Roth, J. Catal. 27 (1972) 389–396.
[12] H.C. Martin, N.H. James, J. Aitken, J.A. Gaunt, H. Adams, A. Haynes, Organometallics 22 (2003) 4451–4458.
[13] D.K. Dutta, J.D. Woollins, A.M.Z. Slawin, A.L. Fuller, B. Deb, P.P. Sarmah, M.G. Pathak, D. Konwar, J. Mol. Catal. A: Chem. 313 (2009) 100–106.
[14] D.K. Dutta, P. Chutia, B.J. Sarmah, B.J. Borah, B. Deb, J.D. Woollins, J. Mol. Catal. A: Chem. 300 (2009) 29–35.
[15] B.J. Sarmah, B.J. Borah, B. Deb, D.K. Dutta, J. Mol. Catal. A: Chem. 289 (2008) 95–99.
[16] D.K. Dutta, J.D. Woollins, A.M.Z. Slawin, D. Konwar, P. Das, M. Sharma, P. Bhattacharyya, S.M. Aucott, Dalton Trans. (2003) 2674–2679.
[17] D.K. Dutta, J.D. Woollins, A.M.Z. Slawin, D. Konwar, M. Sharma, P. Bhatacharyya, S.M. Aucott, J. Organomet. Chem. 691 (2006) 1229–1234.
[18] D. Forster, J. Am. Chem. Soc. 98 (1976) 846–848.
[19] D. Forster, Adv. Organomet. Chem. 17 (1979) 255–267.
[20] D. Forster, T.C. Singleton, J. Mol. Catal. 17 (1982) 299–303.
[21] A. Haynes, J. McNish, J.M. Pearson, J. Organomet. Chem. 551 (1998) 339–347.
[22] T. Ghaffar, H. Adams, P.M. Maitlis, A. Haynes, G.J. Sunley, M.J. Baker, Chem. Commun. (1998) 1359–1360.
[23] J. Rankin, A.D. Poole, A.C. Benyei, D.J. Cole-Hamilton, Chem. Commun. (1997) 1835–1836.
[24] L. Gonsalvi, H. Adams, G.J. Sunley, E. Ditzel, A. Haynes, J. Am. Chem. Soc. 121 (1999) 11233–11234.
[25] B. Deb, D.K. Dutta, Polyhedron 28 (2009) 2258–2262.
[26] B. Deb, B.J. Borah, B.J. Sarmah, B. Das, D.K. Dutta, Inorg. Chem. Commun. 12 (2009) 868–871.
[27] B. Deb, B.J. Sarmah, B.J. Borah, D.K. Dutta, Spectrochim. Acta A 72 (2009) 339–342.
[28] I. Vogel, A Text Book of Quantitative Inorganic Analysis: Theory and Practice, third ed., Longmans Green and Co., 1951.
[29] The analysis of rhodium was carried out by gravimetric method in which the rhodium metal complex was converted to metallic rhodium by following steps: The complex was first decomposed by boiling in conc. H_2SO_4/HNO_3. It was then allowed to react with thiourea when black rhodium sulfide was formed which on ignititon gives the oxide. Lastly, the oxide was quantitively reduced by H_2 gas (at elevated temperature) to metallic rhodium and weighted as such.
[30] J.A. McCleverty, G. Wilkinson, Inorg. Synth. 8 (1966) 211–214.
[31] G.M. Sheldrick, Acta Cryst. A 64 (2008) 112–122.
[32] A. Haynes, B.E. Mann, D.J. Gulliver, G.E. Morrison, P.M. Maitlis, J. Am. Chem. Soc. 113 (1991) 8567–8569.
[33] H. Adams, N.A. Bailey, B.E. Mann, C.P. Manuel, C.M. Spencer, A.G. Kent, J. Chem. Soc., Dalton Trans. (1988) 489–496.
[34] B.P. Morgan, R.C. Smith, J. Organomet. Chem. 693 (2008) 11–16.
[35] M. Sakai, H. Hayashi, N. Miyaura, Organometallics 16 (1997) 4229–4231.
[36] B. Deb, P.P. Sarmah, D.K. Dutta, Eur. J. Inorg. Chem. (2010) 1710–1716.